PROJECT REPORT
1999-23

sustainable
forest
management
network

réseau
sur la
gestion durable
des forêts

Advanced Oxidation
Process (AOP),
Especially Photocatalytic

**Cooper Langford, Alex Starosud
and Elena Vaisman**

For copies of this or other SFM publications contact:

Advanced Oxidation Process (AOP), Especially Photocatalytic

by

Cooper H. Langford, Alex Starosud, and Elena Vaisman
Department of Chemistry
University of Calgary
Calgary, Alberta

July 1999

INTRODUCTION TO TWO YEAR REPORT

The project has included two fairly distinct efforts. One has been the evaluation of the effectiveness of photocatalysis for the oxidation of waste streams from pulp mills. This effort has looked at complex mixtures and examined oxidation of both dissolved and colloidal material. One notable result is the observation of fairly efficient treatment of colloidal organics. The second part of the effort which is joint with a project sponsored by Trojan technologies of London, ON and an NSERC U/I grant has been the development of the appropriate supported TiO_2 photocatalysts, and study of reactor design parameters. A notable outcome of this part has been patenting of two photocatalyst formulations by UTI, the U of C technology transfer company, and sale of options on those to Trojan. Both parts of the project have been the subject of public presentations. The first was presented at the Sustainable Forest Management Conference in Edmonton this year. The second was presented at the International Symposium in reaction Kinetics and Development of Catalysis at Brugge, Belgium, April, 1999. The report will follow, with elaboration, the reports made at these meetings.

PART 1

INTRODUCTION

Governments in North America and Europe are beginning to develop a "certified forest product" approach that leads to more stringent requirements on discharges of wastewater from pulp and paper mills. Effective management of wastes is a key component of the "life cycle" dimension of sustainable forest management. To comply with evolving regulatory standards, and to adopt environmental stewardship as corporate responsibility, Canada's pulp and paper industry is encouraged to take the initiative in significant technological innovations.

As always, a waste management process faces the law of conservation of mass and consideration must be given to the fate of the products of a treatment process. If contaminants are removed from the aqueous phase to render water safe for discharge or useable for recycle, an early question is into what phase are they delivered? For example, adsorption and biological treatment create solid waste management problems. The central attraction of advanced oxidation (AO) processes is that organic contaminants are commonly oxidized to CO_2. The relatively small amounts of organic matter, and the ultimate fate that organic matter might experience under other treatment regimes, does not imply a significant contribution to greenhouses gases. Thus, the advanced oxidation processes offer an attractive option to use the gas phase as the carbon sink.

Our research program has addressed the use of advanced oxidation, specifically schemes based on TiO_2 photocatalysis, in treatment of streams in pulp and paper processing. Our concept encompasses both independent use of AO and use of AO as a supplement to conventional biological treatment processes.

Titanium Dioxide Photocatalysis

Solid TiO_2 absorbs light in the near UV, promoting an electron from the valence band (essentially oxide ion orbitals) to the conduction band (essentially Ti ion d-orbitals). The carriers can be trapped at or near the particle surface and undergo electron transfer reactions across the interface with molecules from solution adsorbed on the TiO_2 surface. The trapped carriers have effective solution potentials on the hydrogen scale of +3.2 V for the hole and about 0 V for the electron. Thus, the hole is an extremely powerful oxidizing agent and the electron a good reducing agent. The hole can generate a hydroxyl radical at the surface or initiate one electron oxidation of a very wide range of adsorbed organic molecules. The electron is readily captured by O_2 to give the reactive superoxide ion. Thus, the illuminated surface of TiO_2 is a very attractive catalyst for initiation of oxidation of almost all organic compounds. In most cases, that oxidation can be continued so that the final products are CO_2, H_2O, and inorganic ions of other elements present in the organic molecule (this outcome is termed mineralization). The problems which have limited the widespread commercialization of this attractive technology to date are the material handling problems presented by the fine particulate nature of TiO_2 and the fact that the TiO_2 polar surface is not favorable for adsorption of organics in competition with water. As a

result, no commercial application of TiO_2 photocatalysis to aqueous waste streams has yet emerged.

EXPERIMENTAL SECTION

Materials

The present work examined both synthetic and "real" pulp mill white water samples (MWW) from Howe Sound Pulp and Paper Mill supplied to us by UBC group of Prof. J.N. Saddler. The synthetic white water, called a "model" highly recycled white water (Zhang, 1995), was made from fresh Spruce-Pine-Fir chips obtained from Canadian Forest Product Ltd. Thermomechanical pulp was made from these chips in PAPRICAN's pilot plant using a Sunds Defibrator TMP 300 single disk laboratory refiner. The "model" white water was prepared by washing the TMP with distilled water in a batch process. In each batch, 3.6 kg of pulp was washed with 180 L of distilled water at 60° C for 20 min., with stirring. The pulp suspension was dewatered using a screw press to about 45% consistency and the water was collected as white water. The collected white water was used to wash a fresh batch of TMP in order to obtain a recycled white water. After 5 washes, the "model" white water was collected and referred to as the "highly recycled white water". The MWW contains carbohydrates, lignins, resins and fatty acids, as well as lignans, sterols, steryl esters, and triglycerids. Total concentration of organic matter is 2 - 3%.

Photocatalysts for this research were chosen from a series of catalysts prepared by Dr. A. Starosud in a program conducted in partnership with Trojan Technologies (London, ON). The efforts at Calgary were directed towards the development of an integrated photocatalyst-adsorbent matrix. The integrated matrix approach is a new concept that combines adsorption with advanced oxidation by photocatalysis. There is an additional opportunity to gain in photocatalytic efficiency since the problem of encounter of substrate with the photoactive site is reduced from three-dimensional to two-dimensional diffusion. However, the high organic content of the white waters did not require the high adsorption capacity of some of the new catalysts. The optimum catalyst in our series proved to be the "UC-210" material with TiO_2 (P25) from Degussa loaded on silica gel from Grace Davison. Colloidal silica Ludox HS-40 from Aldrich Chemical Company was used as a solvent. The advantage of the UC series materials is that they retain TiO_2 reactivity while being based on an inexpensive core that makes them attractively low cost. A parallel unsupported TiO_2 (P25) powder was also used throughout this study to compare with the supported samples.

Photolysis procedures

Preliminary experiments were performed in sealed test tubes containing 30ml of slurry and a head space of approximately 2ml that were rotated under a 40 W fluorescent bulb with emission centered at 350 nm. The light source had an average intensity 4×10^{-8} einsteins /s. A flow cell (

similar to a fluidized bed reactor) in a Rayonet reactor from Southern New England Nuclear was implemented next. In this latter case, the photocatalyst was retained in the cell by glass wool and centered within the irradiation zone consisting of a ring of 16 75W fluorescent coated Hg tubes which emitted light centered at 350 nm. The average intensity in the cell was 1.5×10^{-7} einsteins /s. The volume of the reaction zone was 10 ml and a total volume of 250 ml of solution was circulated in the flow reactor.

For comparison, some photolysis runs were conducted using UV / H_2O_2 scheme. In these experiments, different amount of H_2O_2 (from 0.1% up to 5% of the sample volume) were added directly into the test tube or into the flow cell where the mixture of MWW and H_2O_2 underwent similar to above mentioned irradiation. Finally, a combined scheme using small initiating amounts of H_2O_2 with UC-210 was explored. A mixture of 0.2g UC-210, 0.5% H_2O_2, and MWW sample was irradiated the same way to compare with previous experiments.

Analytical methods

High Performance Liquid Chromatography (HPLC) has been employed for monitoring photoproducts and intermediates. The instrument was Water 600 with C_{18} column operated under the following conditions: wavelength of UV detector set up at 240 nm, 50:50 mixture of CH_3CN and H_2O used as eluent with flow rate equal to 1.00 ml / min.

The effectiveness of photodegradation of organics was evaluated by comparing chromatograms before and after timed irradiation intervals, to ascertain any changes. Aliquots of 1 ml were drawn from the sample solution and 20µl was injected. Since the samples are complex mixtures, the chromatograms do not provide detailed information about the composition of MWW. However, they provide valuable qualitative information such as indicating differences in degradation pathways under different reaction conditions. As well, disappearance of certain reactant peaks and appearance of certain intermediate peaks provide crude approximations for kinetic parameters. The qualitative HPLC approach had to be adopted for analysis of large numbers of runs because a detailed analysis of the composition of the white waters (see below) is too complex to be applied to results from large numbers of runs.

Detailed analysis of colloidal and dissolved substance content on the samples was done at UBC (Zhang, 1995). The white water was extracted with methyl *t*-butyl ether (MTBE) to separate the lipophilic extractives from the highly water solubles (Orsa, 1994). Total dissolved and colloidal substances (TDCS) were measured based on dry weight, by oven-drying the water sample at 105 ± 3° to constant weight. The carbohydrates present in the freeze dried white water samples were measured by HPLC (de Jong, 1997). The lignin content was determined as acid-insoluble lignin of the freese dried extractives free white water sample (Tappi standard method T222). The ash content was measured according to Tappi standard method T211. The extractive groups, resin and fatty acids, lignans, steryl esters, and triglycerides were meadured by gas chromatography (Orsa, 1994). The water surface tension was measured by the capillary method (Shoemaker, 1981).

RESULTS

Qualitative evaluation using rotating tube reactor

HPLC analysis of the irradiated MWW, both synthetic and "real", in the rotating tube indicated that extensive photocatalytic oxidation was definitely taking place at an average light intensity of 4×10^{-8} einsteins /s. Some decolorization of the MWW had been achieved as well. Results of a typical HPLC analysis are shown in Fig. 1. Irradiated samples show a decrease in the more non-polar and an increase in the more polar organics, comparing to the initial MWW. These changes are more obvious with an increase of the photocatalyst loading as shown in Fig. 2.

Since irradiation of waters to which hydrogen peroxide is added is an alternative method for photochemical initiation of oxidation, reactivity using photocatalysts was compared to the H_2O_2 / UV scheme. HPLC analysis showed that both approaches were effective in degrading major components of white water samples, but the pathways were different. This is clearly indicated by the different peak distribution in the chromatograms shown in Fig. 3.

The comparability of reactions with the photocatalyst or peroxide suggested exploration of the effectiveness of a mixed approach. Comparing the chromatograms over specific time-frame (Fig. 4 - 6), although the compounds were not identified, one could notice crucial qualitative differences in the amount of photodegradation occurring among samples irradiated with photocatalyst alone, hydrogen peroxide alone, and in the case of their combination. TiO_2 photocatalysis enhanced by H_2O_2 proved to by significantly superior to either scheme alone. In this case of combined treatment, no more than traces of organics were found in the sample after 6 days of irradiation under 40 W bulb (Fig. 6). Also, the sample completely lost color. Half-life, based on the estimation of the initial component with retention time equal 1.04 min., was approximated as 0.5 day.

Fortunately, it turns out that enhancement of TiO_2 reactions does not require stoichiometric amounts of hydrogen peroxide. Fig. 7 show that the rate of decomposition depends on the amount of H_2O_2 in the mixture and has a maximum at 1 % of H_2O_2. With less amount of H_2O_2, the reaction goes slower, but when the concentration of hydrogen peroxide is bigger than 1%, it seems to suppress further destruction of the components. Moreover, further additions of H_2O_2, after a time for the initial small charge to be consumed, does not produce any increase on reactivity in the presence of the photocatalyst. Fig. 8, 9 show that everyday injections of hydrogen peroxide, being a continuous source of new hydroxyl radical, lead to the formation of the biggest amount of a component with retention time equal 1.15 min but these injections also prevent this component from further destruction. Fig. 9 also shows that interruption of H_2O_2 injections allows this component to degrade as before.

Thus, H_2O_2 functions as an initiator only at the outset of irradiation. A main limit of the H_2O_2 technology is the cost of hydrogen peroxide. Since only a small initiator addition is required in the presence of the photocatalyst, cost of its use can remain low.

A remarkable feature of figures 4-6 is that, once again, the pattern of peaks for TiO_2 photocatalysis enhanced by H_2O_2 is novel. The pathway of oxidation is not equivalent to either that with UC-210 acting alone, or H_2O_2 acting alone. Comparing the action of hydrogen peroxide alone with that with the combined approach, one can notice that the intermediate component with retention time equal 1.15 min was produce in both cases during very first day of irradiation but then, it behaved differently over time. In the latter case, this component concentration went through the maximum on a second day of irradiation and later decrease to almost zero after 6 days of irradiation, while in the former case this component, once formed, didn't seem to decompose even after 10 days of irradiation. Taken together, these experiments suggest an organic chain mechanism of oxidation that is taking place. The hydrogen peroxide acts as a initiator, which generates organic radicals, which then react with intermediates from photocatalyzed oxidation to generate a radical chain and faster overall oxidation.

To compare the reactivity of supported TiO_2 with unsupported commercial titania, experiments have been made with P25 TiO_2 alone as well as in combination with hydrogen peroxide (Fig. 10, 11). Apparently, substitution for the unsupported P25 did not change the pathways described earlier for the correspondent reactions with supported titania However, at initial stage, photocatalysis of MWW was faster with unsupported TiO_2, although it can be explained by the presence of a larger amount of photocatalyst. Since equal loading of catalysts were used throughout the experiments, the real concentration of unsupported TiO_2 was 20 times more then for the supported TiO_2. But the initial extent of photodegradation by unsupported TiO_2 has not been significantly increased over a time of the irradiation while supported TiO_2 left only traces of organic after 6 days of irradiation. It's worth mentioning that unsupported TiO_2 itself became very dark at the end of the experiments which can be explained by contamination of its surface that prevent it from further activity.

Product analysis from flow reactor

Flowing samples were irradiated in the Rayonet based flow reactor for up to 96 hours using the combined UC-210 / H_2O_2 scheme in comparison to use of UC-210 alone and 1% H_2O_2 alone. Detailed analyses, which characterize the major components of the white water, were performed at UBC on the final samples from these runs. The results confirm successful mineralization of dissolved and colloidal substances in white water samples. The successful oxidation of colloidal material is an especially important result since it might be assumed that only dissolved organic matter could reach reactive sites on the solid state photocatalyst. Results of analyses, where "%" represent degree of loss of each of the important classes of the input stream treated in a Rayonet system for 96 hours, are collected in Table 1.

Table 1. Analyses of samples from treatment of Mill White Water from Howe Sound mill in flow reactor for 96 h.

Contaminant	Initial MWW mg / L	UC-210 mg / L	%	1% H_2O_2 mg / L	%	UC-210+1% H_2O_2 mg / L	%
Total dissolved & colloid organics	2360	1120	48	340	14	160	7
Lignin	100	80	80	7.5	7.5	15	15
Ash	390	213	55	163	42	67	17
Carbohydrates	1560	670	43	n / d	0	n / d	0
Extractive resins & fatty acids*	14	20.5	146	58.3	416	15.4	110
Sterols & Lignans	88	34.3	39	26.6	30	16.4	19
Steryl Esters & Triglycerids	16	12.3	77	11.3	71	9.9	62

* There is noticeable early production of resins and fatty acids from larger MWW substances although the extent is quite different in the different cases.

CONCLUSIONS

The experiments to date clearly demonstrate that photocatalysis using UC-210 can achieve oxidation of both dissolved and colloidal organic matter in a white water system at interesting rates. Reported almost complete photodegradation of organic matter in MWW achieved after 6 days at an average light intensity of 4×10^{-8} einsteins /s corresponds to approximately 10 hours of sun exposure at a sunny day. Color reduction can also be achieved.

We foresee two points in current mill operation where it will be of interest to design a photochemical reactor. One is for the acid stream. This will require a high rate configuration with high intensity UV lamps. The other is as a supplement and enhancement of treatment ponds. Pond residence times are long enough to allow consideration of solar radiation as the light source.

ACKNOWLEDGMENTS

REFERENCES

de Jong, E., Wong , K.K.Y., and Saddler, J.N. 1997. The Mechanism of Xyianase Prebleaching of Kraft Pulp: An Examination Using Model Pulps Prepared by Depositing Lignin and Xylan on Cellulose Fibers. Holzforschung 51(1): 19-26.

Orsa, F., and Holmbom, B. 1994. A Convenient Method for the Determination of Wood Extractives in Papermaking Process Water and Effluents. J. Pulp Paper Sci., 20(12): J361-366.

Shoemaker, D.P.,Garland, C.W., Stinfield, J.I., and Nibler, J.W. 1981. Experiments in Physical Chemistry. 4-th ed., McGraw-Hill, New York. pp. 329-331.

Zhang, X., Cai, Y., Stebbings, D., Beatson, R.P., and Saddler, J.N. 1995. Influence of Accumulated Dissolved and Colloidal Substances on Paper Properties and the Potential of Enzyme Treatment for Component Removal. In Enzymic Degradation of Insoluble Carbohydrates. Saddler, John N.; Penner, Michael H.; Editors. ACS: Washington, D.C., Eng. pp. C151 - C154.

INTRODUCTION

Heterogeneous photocatalysis offers an attractive alternative for wastewater treatment especially when treating low concentration high volume fluids. For the photocatalytic process, the most suitable semiconductor is TiO_2. It is characterized by chemical inertness, nonphotocorrosivity,and nontoxic influence on microorganisms. These properties, coupled with its ability to create highly reactive oxidant (hydroxyl radical) on excitation with UV radiation make titanium compounds highly suitable for application in wastewater treatment. The hydroxyl radical (OH•) which is known to be one of the most powerful oxidizing species, mineralizes organic pollutants to carbon dioxide and inorganic ions. This technology has been developed and it is currently being evaluated for application at pilot plant and semi-industrial scales of testing.

The efficiency of photocatalytic reactors using immobilized photocatalysts have been found to be lower than those using dispersed titania particles (slurry).

Application of fine powder of TiO_2 is technologically impracticable because powders could be easily washed out. To prevent this phenomenon, it is necessary to construct additional equipment [1] which causes a sharp rise in the cost of the process.

There is a rigid practical necessity to immobilize titania [1,2]. Many attempts have been made using glass beads, fiber glass, silicon, quartz, activated carbon and zeolites as support [1,2,3].

PHOTOCATALYST SYNTHESIS

Zeolites, as a catalyst support, offer the advantage of having high adsorption for organics in wastewater aiding preconcentrating of pollutants on their surface.

More than 40 different types of zeolites and their modifications were synthesized and tested as supports. All of the synthesized materials can be divided in four classes:
1. Mesoporous molecular sieves (MCM-41) and relatives.
2. Titanium silicates (TS class with Ti incorporated into zeolite lattice) of both micro and meso pore types.
3. Aluminophosphates sieves (VPI-5 and relatives) containing both Si and Si-Ti .
4. Siliceous zeolites of the MFI and MEL structure families (TS-16, ZSM 48, etc.).

PHOTOCATALYST EVALUATION

Adsorption characteristics of all synthesized materials were evaluated using static conditions. The static experiments involved slurrying the material into solutions of organic contaminants for periods up to 48 hours. The aliquot and filtrate were analyzed by HPLC or GC.

Most of these synthesized zeolites exhibited relatively low adsorption toward chosen contaminants as compared to activated carbon as a standard. Some results for Isopronanol (IPA) acetone and 2,4 - dichlorphenol are given in Figure 1 for the most promising materials.

The major rival for zeolite materials is activated carbon. From Figure 1, it can be seen clearly that two of our materials (163ARC and TS-16) have nearly the same capacity as carbon and are even superior toward polar contaminants (acetone, IPA).
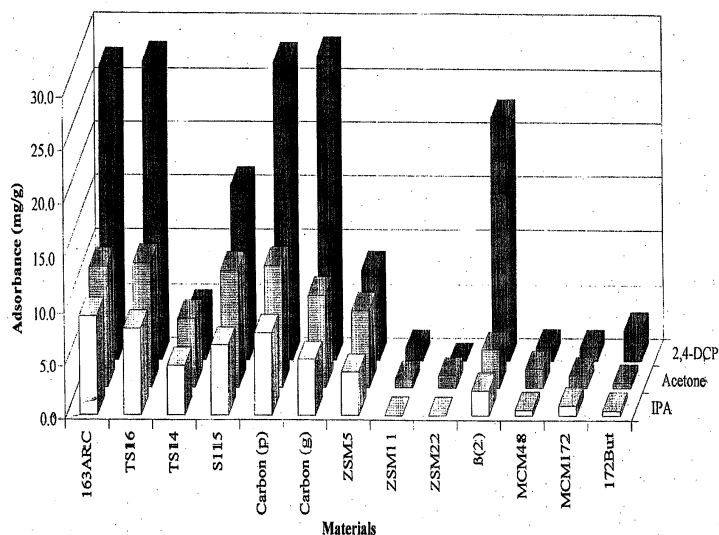
Figure 1. Static Adsorption of Organics on Zeolite Materials

The most interesting zeolites were loaded with titania to obtain an integrated photocatalyst-adsorbent system (IPCA).

TiO_2 loading was accomplished by stirring the zeolite with a previously prepared colloid of TiO_2 , evaporating the solvent, and calcining the resultant solid at a temperature between 200 °C and 500 °C. This was the preferred method of TiO_2 loading which has been identified in earlier work [4]. Two modifications were also used. First, the standard colloid with particle size in 10 nm and higher range were replaced with a preparation of "quantum size" or "Q-sized" particles of 2-4 nm size [5]. A further modification with loading Q-sized particles under these conditions, in this case filtration, replaced evaporation of solvent.

Physical characterization of IPCA has included Raman spectroscopy to examine the state of TiO_2, SEM to identify TiO_2 clustering, and XRD to verify the identity of the zeolite phases and

the apparent particle size in TiO$_2$ loading. An interesting result is that all TiO$_2$ reflections in XRD have line width suggesting particle size smaller than the size of colloidal TiO$_2$ particles used in loading onto the support. This led us to question the TiO$_2$ distribution.

A novel energy filtered transmission electron microscopy technique was developed to obtain a Ti distribution map [6]. It was found that whenever zeolite pores are smaller than the particle size of TiO$_2$, the colloidal particles used in loading titania remains on the surface.

For general screening of photocatalytic behavior of IPCA, a larger diameter Teflon cell with a quartz window at the top was used. Several of these could be irradiated simultaneously under a pair of 40W fluorescent UV lamps with peak output at 350 nm. Substrate oxidation was measured using a mass balance approach where reduction of solution concentration was monitored and IPCAs were extracted with organic solvent at the end of runs to recover any material adsorbed.

The overall results of screening for photocatalytic activity can be summarized as follows:
1. a "classical" MCM-41 exhibited higher activities than zeolite Y (used as a reference);
2. titanium silicates showed very low activity;
3. silicon and titanium containing aluminophosphates had low activity;
4. several members of MFI and MEL families were quite active.

Unfortunately, the adsorption characteristics of MCM-41 class are not satisfactory, so emphasis turns to MFI and MEL family of materials. Several locally synthesized systems including ZSM-48, ZSM-11 and TS-16 are very promising. As well, commercial ZSM-5 and silicalite I are competitive. In order to reduce the cost of the IPCA, a new approach has recently been developed. The general idea was to use inexpensive and readily available particles with a desired diameter as a carrier for titania and zeolite. The general idea was to use inexpensive and readily available particles with desired diameters (200 – 700 mk) as a carrier for titania and zeolite. The carrier has to be mechanically strong, not reduce photoactivity, and have a "golf ball" like surface to reduce attrition of zeolite/titania which may be "sheltered" by depressions. We used silica gel 210-104 with particle size of 200-700 mm (supplied by Trojan Technologies). The entire procedure looks straightforward : binder (colloidal silica, sodium silicate or a blend of the two) is mixed with a defined amount of TiO$_2$ and zeolite to provide adsorption capacity for organic contaminants, then the mix is filtered through or slurred with silica gel. The dried material is ready to use as an IPCA. In case of using liquid sodium silicate as a binder, the series is given the name UC-100, if a binder is colloidal silica, the name is UC-200 (e.g. UC-210 used in Part I), and if a binder is a blend, the name is in the UC-300 series. The adsorption capacity of these materials toward DCP is about 50% of the value found for one of the best zeolites (ZSM-5, TS-16, ARC-163), but the cost has been reduced by a factor of 4-5.

In the case of treatment of pulp mill wastes, it was found that moderate adsorption capacity was an advantage. If a UC catalyst with high adsorption capacity was tested, coagulation of the colloidal organics in the stream was a problem for treatment. Thus, a relatively low

adsorption capacity catalyst (UC 210) was described in Part I as the most useful for the pulp mill white waters. However, we have the capacity to tune catalysts to specific streams from the repertoire now available.

PHOTOCATALYTIC REACTOR

Reactor Design and Construction

For heterogeneous photocatalytic reactions the contact among reactants, photons and catalysts must be maximized. Mixing and flow characteristics of the photoreactor may greatly enhance these contacts. If a fixed bed reactor is used, the irradiated aliquot of catalyst is limited to a thin layer and a large reactor volume is required. For the liquid-solid and gas-solid systems, continuously stirred tank photo reactors and fluidized bed photo reactors, respectively, are the most suitable ones for enhancing contact efficiency even if their operation is quite expensive and troublesome. The rate of photocatalytic reaction is greatly affected by flow rates. The rate enhancement is not due to elimination of mass transport resistances, as expected in classical catalytic systems, since such considerations do not apply for most heterogeneous photo-processes that are characterized by low reaction rate with respect to mass transport rate. The enhancement is determined by the fact that on increasing flow rates, the frequency of exposure of the catalyst particles to irradiation increases. The catalyst particles continuously receive diffuse radiation of reduced intensity due to absorption by other catalyst particles. They are directly irradiated intermittently due to shielding effect of particles which randomly intercept direct irradiation. By increasing flow rates, the frequency with which the catalyst particles may be directly irradiated increases and eventually, the reaction rate is enhanced.

With the above considerations, an annular liquid fluidized bed photocatalytic batch reactor with full recirculation was constructed. A schematic of the reactor showing the adsorption and regeneration cycles is depicted in Figure 2. The above reactor was then modelled based on the study done by Rideh *et. al.* [7]. In this kind of reactor, the extended light source is placed at the axis of a reactor composed of two coaxial cylindrical tubes. The emitted radiant power is absorbed by the reaction system contained in the annular reactor volume. Irradiance diminishes in a filled reactor with increasing radius. This geometry called the negative geometry of irradiation makes the most efficient use of the light emitted by an extended light source. In fact, this geometry is used in all immersion type photochemical reactors, and most industrial photochemical production units [10].
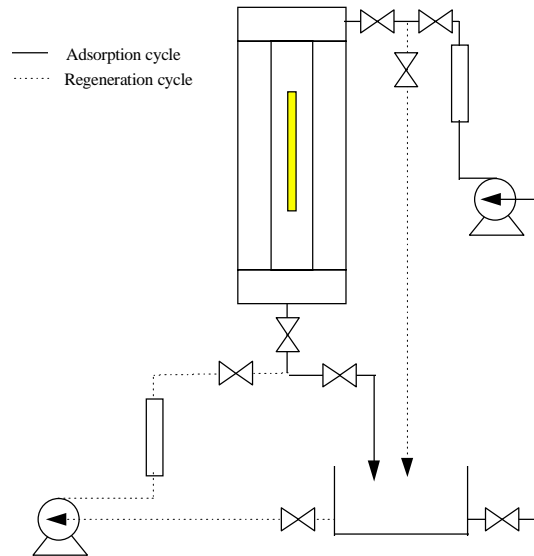
Figure 2. Schematic diagram of the photocatalytic reactor

Photocatalytic Reactor Modelling

The purpose of this study was to model and simulate a liquid fluidized bed photocatalytic reactor for 2-Chlorophenol degradation operating in once through and dual mode (adsorption followed by regeneration). Also, to analyze the effect of various operational parameters such as initial pollutant concentration, flow rate, oxygen partial pressure, absorbed UV light intensity, initial bed height using the developed simulator with a view to find out the range of operational parameters for optimum reactor performance.

Hydrodynamic Modelling

A hydrodynamic model was set up using the Wen and Yu Correlation [8] to predict the bed voidage as a function of superficial velocity. The number of particles in the elemental volume under consideration were calculated using geometry. We could arrive at the average light intensity reaching a photocatalyst particle surface using the line source with parallel plane (LSPP) emission model [9]. In this model, the lamp is considered to be a linear source in which each point emits radiation in parallel planes perpendicular to the lamp axis. Combining this hypothesis with the Beer-Lambert equation, the integration of the differential equation describing the radiant power or irradiance as a function of the optical path yields the profile of radiant power or irradiance.

Kinetic Modelling

Kinetic modeling of the primary degradation steps is essential for any practical application of the process. Rideh *et al.* [7] showed that 2 - Chlorophenol was degraded in an illuminated suspension of TiO_2 according to the following stoichiometry:

$$2C_6H_4OHCl + 13O_2 \xrightarrow{TiO_2/h\upsilon} 2HCl + 12CO_2 + 4H_2O$$
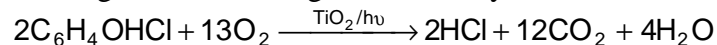
Model Assumptions

12

A pseudo-plug flow model has been used to simulate the process. A number of discrete plug flow reactors of an annular shape have been considered to represent the reactor. The assumptions used in the development of model are:

1. Complete radial mixing and no axial mixing in the elemental volume.
2. No mixing between the adjacent annular PFR's.
3. No reaction in the part of the reactor above the expanded bed (i.e., no direct photolysis).
4. Even distribution of photocatalyst particles in the expanded bed region.
5. Same inlet concentration to all the annular PFR's.
6. Complete mixing of the wastewater while effluent is recirculated.

Model Development
Prediction of Absorbed Light Intensity

Total number of particles in the reactor can be calculated from the voidage and height of bed at minimum fluidization :

$$N_P = \frac{3}{4} \frac{\left(1 - \varepsilon_{mf}\right)\left(R_O^2 - R_I^2\right)H_{mf}}{r_P^3}$$

Particle number density in the expanded bed region can be calculated from the total number of particles in the reactor, assuming equal distribution of particles in the expanded bed region.

$$N_{PD} = \frac{N_P}{\pi\left(R_O^2 - R_I^2\right)H_{EX}}$$

Where, the expanded bed height is calculated from the voidage predicted by Wen & Yu Correlation :

$$H_{EX} = \frac{\left(1 - \varepsilon_{mf}\right)}{\left(1 - \varepsilon\right)} H_{mf}$$

Thus, number of particles in the elemental volume can be calculated as :

$$n_P = N_{PD}\pi\left(R_O^2 - R_I^2\right)\Delta z$$

The light intensity incident to elemental volume under consideration is given by the LSPP Emission Model :

$$I_{Inc} = \frac{S_{L;\lambda} \exp[-\mu(r - R_I)]}{\pi(R_o^2 - R_i^2)}$$

Hence, the net light intensity absorbed by the photocatalyst particles present in the elemental volume is given by :

$$I_{Abs} = \frac{I_{Inc} n_P \pi r_P^2}{2\pi r \Delta z}\alpha\beta$$

where,
α = fraction of particles which are irradiated by the incident photons.
β = fraction of incident light intensity absorbed.

Material Balance for Once Through Process

Material balance based on the amount of pollutant (2-Chlorophenol) inside the elemental volume can be written at steady state as follows :

[Mass of 2-CP in] - [Mass of 2-CP out] - [Mass of 2-CP degraded by photocatalysis] = [Accumulation]

At steady-state, [Accumulation] = 0.

Also,

[Mass transfer of 2-CP from bulk to photocatalyst surface] = [Mass of 2-CP degraded by photocatalysis]

$$Q.(C_i)_{r,z} - Q.(C_i)_{r,z+\Delta z} = A.\Delta z.(rate)$$

$$\frac{dC_i}{dz} = -\frac{(rate)}{U_L}$$

$$\int \frac{dC_i}{(rate)} = -\frac{1}{U_L}\int dz$$

where, the rate expression is evaluated in the same manner as Rideh *et al*.[7].

Material Balance for Dual Mode Process

A similar material balance conducted for 2-CP in the bulk liquid and solid catalyst phase results in a set of ordinary differential equations.

For bulk liquid phase :

$$\frac{dC_L}{dz} = \frac{1}{u}\int k_L a(C_S - C_L)$$

For solid catalyst phase :

$$\frac{dC_S}{dz} = -\int \frac{A}{W}\left[k_L a(C_S - C_L) + k_r' k' I_{abs} C_{O_2}^n C_S \right]$$

The liquid-solid mass transfer coefficient was evaluated using the correlation proposed by Hassanien *et al*. [11]:

$$Sh = 0.33(Ga.Mv.Sc)^{1/3}[1 + 0.22 Mv^{-0.57}(U_G / U_L)^{0.77}]$$

Solution of Model Equations

The material balance conducted for the pollutant in the liquid and solid phase in a PFR over the elemental volume at a fixed radial distance resulted in a set of simultaneous first-order ordinary differential equations. The equations were solved numerically using fourth order Runge-Kutta method with adaptive step-size control to obtain 2-CP concentrations at various axial distances. The above steps were carried out for all the annular PFRs. The values of 2-CP concentrations obtained at the outlet of the reactor were then averaged and formed a new initial concentration to the inlet of the reactor for the next time step. The same procedure was repeated for a number of circulations to obtain 2-CP concentrations at the outlet of the reactor corresponding to time. For the adsorption cycle, break-through of the photocatalyst bed was considered when more than 95 % of it was saturated. For the regeneration cycle, bed was considered as regenerated when 99 % of the initial adsorbed concentration was removed from the solid phase due to reaction or transfer to the bulk liquid phase.

RESULTS AND DISCUSSION

The dimensions and process variables required as an input for the simulations are presented in Table 1.

Table 1. Dimensions and process variables

Parameter	Value
Mean particle diameter	500 microns
Particle density	3000 kg/m^3
Sphericity of particles	0.67
Viscosity of water @ 25°C	0.001002 kg.m/s
Density of water @ 25°C	998.2 kg/m^3
Molar absorption coefficient	0.01
Reactor length	0.80 m
Inner radius of the reactor	0.06 m
Outer radius of the reactor	0.10 m
Initial bed height	0.45 m
Voidage at min. fluidization	0.49
Oxygen partial pressure	0.575 atm
Recirculation flow rate (regeneration cycle)	27 lpm
Superficial velocity	0.0224 m/s
Residence time	0.595 min.
Power emitted by source	1.98×10^{-5} Einstein/m.sec.
α (Fraction of particles incident to light)	0.50
β (Fraction of incident light absorbed)	0.75

The model for once through process was run using the above process variables and dimensions. The effect of initial concentration on 2-CP degradation was studied by maintaining the water recirculation rate at 27 lpm (when bed is fully expanded) and the initial 2-CP concentration was varied from 0.0003 to 0.004 mol/L. The effect of oxygen partial pressure on 2-CP degradation was studied by maintaining the water recirculation rate at 27 lpm and an initial 2-CP concentration of 0.0005 mol/L. The results of simulations for the once through process are presented in graphical form in Figures 3 and 4. The trends obtained with respect to the effect of initial concentration and oxygen partial pressure on 2-CP degradation satisfactorily match those obtained by Rideh et al. [7]. However, the values obtained do not match perfectly due to the following reasons : (a) our reactor was much larger than theirs (b) they used the power emitted by the radiation source measured by uranyloxalate actinometry whereas a LSPP model was used in our study to arrive at the light intensity in a particular volume element under consideration (c) difference in the photocatalyst properties such as particle size, particle density, etc.
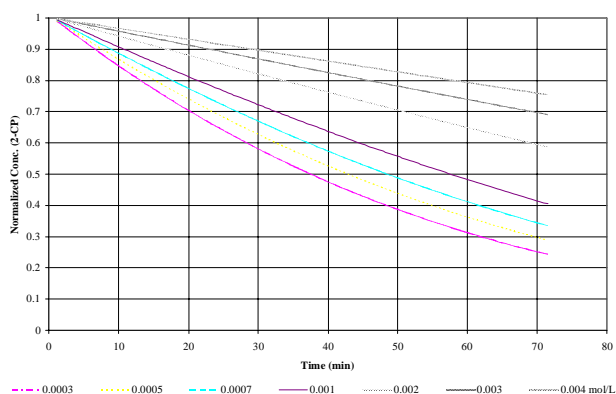
Figure 3. Effect of initial concentration on 2-CP degradation
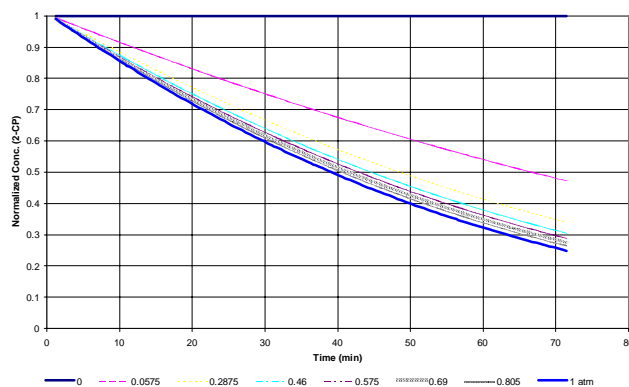
Figure 4. Effect of oxygen partial pressure on 2-CP degradation

For studying the effect of operational parameters in dual mode process, the range of values of various operational parameters used in simulations are presented in Table 2.

Table 2. Range of values of operational parameters

Parameters	Values
Water recirculation rate	9 - 42 L/min.
Oxygen partial pressure	0.0575 - 1.0 atm
Power emitted by source	(3.96×10^{-6}) - (9.9×10^{-5}) Einstein/m.sec.
Initial bed height	0.1 - 0.65 m
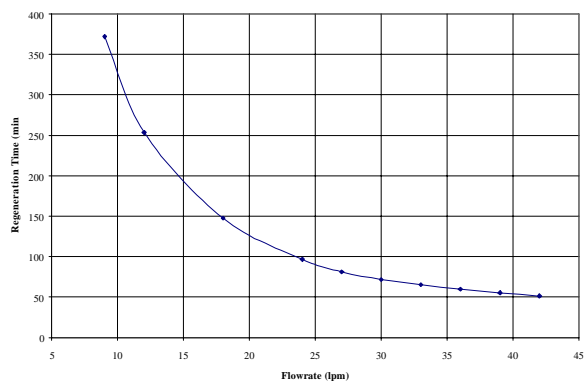
Figure 5. Effect of flow rate on regeneration time
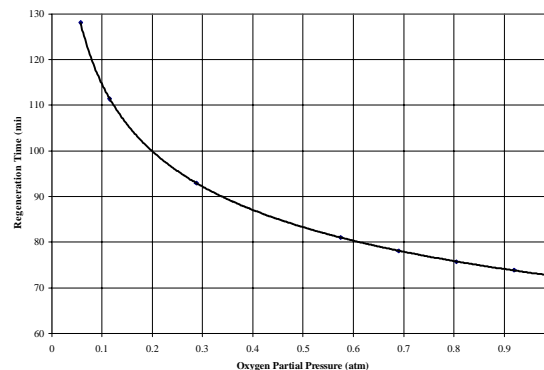
Figure 6. Effect of oxygen partial pressure on regeneration time

The effect of varying water recirculation rate on regeneration time is depicted graphically in Figure 5. There is a pronounced drop in regeneration time required when the flow rate is increased to a value where the bed is fully fluidized, this is because of the fact that on increasing flow rates, the frequency of exposure of particles to irradiation increases. Also, the height of bed exposed to irradiation increases and the decrease in particle density facilitates more effective capture of the incident radiation. The decrease in regeneration time is not so pronounced once the

16

bed is fully expanded at a flow rate of 27 lpm, as the only beneficiary factor is the increase in frequency of exposure.

According to Figure 6, there is a sharp nonlinear decrease in the regeneration time on increasing the oxygen partial pressure. It confirms the fact that the partial pressure of oxygen is a crucial factor in the photocatalytic reaction and the limitation of the rate of photocatalytic degradation is attributed by most researchers to the recombination of photogenerated electron-hole pairs. Since, oxygen adsorbed on titanium dioxide surface prevents the recombination process by trapping electrons, it can be inferred that the reaction rate is a function of the fraction of adsorption sites occupied by oxygen. Hence, oxygen adsorption becomes a governing factor at very low dissolved oxygen concentrations.
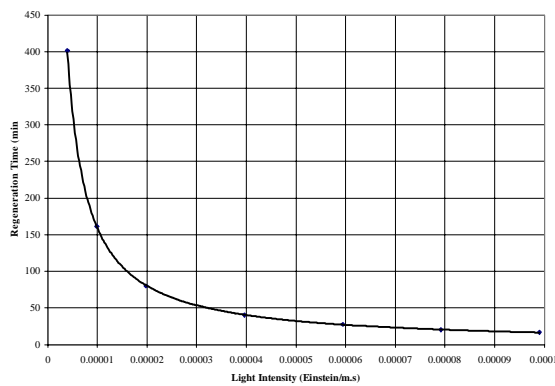
Figure 7. Effect of light intensity emitted by source on regeneration time
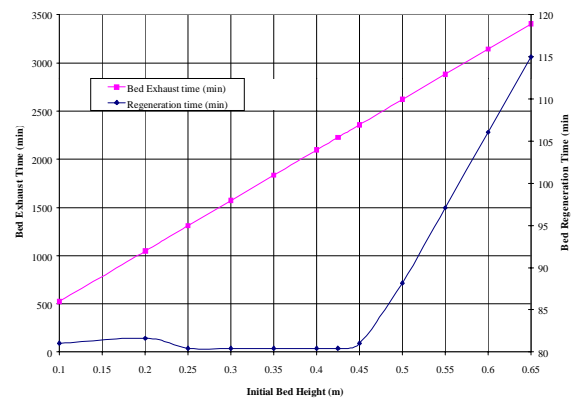
Figure 8. Effect of initial bed height on regeneration time and bed exhaust time

Results reported in Figure 7 show an exponential decrease in the regeneration time required with an increase in the light intensity. The slope decreases after a certain value when it approaches saturation of the catalyst by the incident photons. Since, the annular irradiated thickness is quite large in the reactor, it requires a very high intensity lamp to reach saturation. A trade-off depending on the lamp availability and its power requirement has to be investigated to optimize reactor performance.

Simulations were carried out to study the effect of initial bed height on regeneration time and bed exhaust time, keeping the flow rates in both the modes constant at 27 lpm and a pollutant concentration of 0.0005 mol/L in the adsorption phase. The results shown in Figure 8 depict that there is a linear dependence of bed exhaust time with initial bed height and the slope will depend upon the flow rate and pollutant concentration in the adsorption cycle. The regeneration time is around 80 min. and remains about the same for initial bed heights of up to 0.4 m and then increases linearly for higher initial bed heights. The water recirculation rate of 27 lpm suffices to raise the initial bed height of 0.45 m to full expansion. The bed exhaust times are more than ten times higher than regeneration times: so, there is a possibility of increasing the flow rates in adsorption by a factor of ten. This can serve to equalize the bed exhaust and bed regeneration

times which will facilitate continuous operation of two units in parallel, one in adsorption and the other one in regeneration phase, switching over from one to another.

CONCLUSION

Computer simulations on a novel photocatalytic reactor configuration reveal the possibility of using such a system for purification of water containing organic contaminants.

NOMENCLATURE

2-CP	2-Chlorophenol		LSP	Line Source with Parallel Plane
ε_{mf}	voidage at minimum fluidization		P	
$\mu_{\lambda,c}$	molar absorption coefficient		Mv	density number
r	radial distance, m		N_P	total number of particles in the reactor
α	fraction of particles irradiated by incident photons		n_P	number of particles in elemental volume
			N_{PD}	particle number density, particles/L
A	annular cross-sectional area, m^2		Q	flow rate, L/s
β	fraction of incident light intensity absorbed		R_i	inner radius of an annular photochemical reactor, m
C_i	pollutant concentration, mol/L			
C_L	pollutant concentration in bulk liquid phase, mol/L		R_O	outer radius of an annular photochemical reactor, m
C_S	pollutant concentration on solid surface		r_P	mean particle radius, m
Ga	Galileo number		Sc	Schmidt number
H_{EX}	expanded bed height, m		Sh	Sherwood number
H_{mf}	bed height at minimum fluidization, m		$S_{L;\lambda}$	photon rate of the light source per unit length, Einstein/m.s
I_{abs}	absorbed light intensity, Einstein/L.s			
I_{inc}	incident light intensity, Einstein/L.s		U_G	superficial velocity of gas, m/s
k_L	mass transfer coefficient		U_L	superficial velocity of liquid, m/s
K_{2-CP}	adsorption constant for 2-CP			

REFERENCES

Bellobono, I.R., A. Carrara, B. Barni, A. Gazzotti, J. Photobiol. A: Chem., 84 (1994), 83.

Braun, A.M., L. Jakob, E. Oliveros, and C.A.O. Nascimento, Advances in Photochemistry, **18** (1993), 235.

Choi, W., A. Termin, M.R. Hoffman, J. Phys. Chem., **98** (1994), 13669.

Davis, A.P. in "Process Engineering for Pollution control and waste minimization", N.Y., 1994.

Haarstrick, A., O.M. Kut, E. Heinzel, Environ. Sci. Technol., 30 (1996), 817.

Harris, P.R. and J.S. Dranoff, AIChE J., **11** (1965), 497.

Hassanien, S.M., H. Delmas, and J.P. Riba, Entropie, **119** (1984),17.

Rideh, L., A. Wehrer, D. Ronze, and A. Zoulalian, Ind. Eng. Chem. Res. **36** (1997), 4712.

Starosud, A., D.P. Bazett-Jones, Cooper H. Langford, Chem. Com. (1997), 443.

Wen, C.Y., and Y.H.Yu, Fluid Particle Technology, Che. Eng. Prog. Symp. Ser., **52** (1966), 100.

Xu, Y., Cooper H. Langford, J. Phys. Chem., **99** (1995), 11501.